

Automatic change detection using mobile laser scanning

M. Hebel*, M. Hammer, M. Gordon, M. Arens

Fraunhofer Institute of Optronics, System Technologies, and Image Exploitation IOSB,
Gutleuthausstr. 1, 76275 Ettlingen, Germany

ABSTRACT

Automatic change detection in 3D environments requires the comparison of multi-temporal data. By comparing current data with past data of the same area, changes can be automatically detected and identified. Volumetric changes in the scene hint at suspicious activities like the movement of military vehicles, the application of camouflage nets, or the placement of IEDs, etc. In contrast to broad research activities in remote sensing with optical cameras, this paper addresses the topic using 3D data acquired by mobile laser scanning (MLS). We present a framework for immediate comparison of current MLS data to given 3D reference data. Our method extends the concept of occupancy grids known from robot mapping, which incorporates the sensor positions in the processing of the 3D point clouds. This allows extracting the information that is included in the data acquisition geometry. For each single range measurement, it becomes apparent that an object reflects laser pulses in the measured range distance, i.e., space is *occupied* at that 3D position. In addition, it is obvious that space is *empty* along the line of sight between sensor and the reflecting object. Everywhere else, the occupancy of space remains *unknown*. This approach handles occlusions and changes implicitly, such that the latter are identifiable by conflicts of empty space and occupied space. The presented concept of change detection has been successfully validated in experiments with recorded MLS data streams. Results are shown for test sites at which MLS data were acquired at different time intervals.

Keywords: Laser scanning, LiDAR, 3D, MLS, ALS, change detection, multi-aspect, multi-view, multi-temporal

1. INTRODUCTION

Automatic identification of structures within a 3D environment and the analysis of their changes are important steps to provide a basis for planning and monitoring. Common tasks in this context are, for instance, documentation of urban development, surveying of construction sites, or inspection after natural disasters. Military applications include threat-detection in MOU scenarios, convoy protection and counter-IED operations, as well as battle damage assessment.

Photogrammetry and remote sensing offer flexible techniques for contactless observation of a 3D scene with varying geometric resolution and coverage by using different platforms (terrestrial, airborne, space-borne). In addition, change detection requires the acquisition and comparison of multi-temporal data. The temporal resolution of multi-temporal data typically depends on the technical conditions of the involved platforms and sensors which cover a broad field, e.g. from terrestrial observations using a mobile video camera with a frame rate of some milliseconds up to observation from satellites with a revision interval of some days. In the field of remote sensing, the topic *change detection* is discussed very often on the basis of 2D data (images). In contrast to this, in this paper change detection is addressed on the basis of 3D data acquired by mobile laser scanning (MLS).

1.1 Disadvantages of image-based 2D change detection

Change detection has been well studied for surveillance systems that use stationary cameras or moving cameras with nearly the same viewpoint (e.g., nadir-looking aerial photography). Even under these conditions, image-based change detection is a difficult problem, since image features used for comparisons are often dependent on the illumination of the scene, which varies extremely depending on the time of day and the weather conditions. If views from different viewpoints need to be compared, image-based change detection is even less reasonable. Although techniques exist to reconstruct 3D information from image sequences (e.g., VSLAM), within single images, the 2D projection of the information for different viewpoints results in completely different arrangement and perspective distortion of the data (cf. Fig. 1).

*marcus.hebel@iosb.fraunhofer.de; phone +49 7243 992-323; fax +49 7243 992-299; www.iosb.fraunhofer.de



(a) Downtown Vancouver, view from Burrard Bridge, June 2010.



(b) Downtown Vancouver, view from Kitsilano, June 2014.

Figure 1. Difficulty of image-based change detection: two views of Downtown Vancouver at different times (2010/2014) and from different viewpoints. How to detect changes?

1.2 Advantages of 3D data analysis for object recognition and change detection

In contrast to classical methods of image processing, the analysis of 3D data does not require any reconstruction of the geometry of 3D objects, as this information is inherently included in the data. Object recognition and change detection in 3D data are further supported by the fact that the segmentation of the data and the evaluation of shape features can be performed independent of lighting conditions and color contrasts. Acquisition and analysis of 3D data are of increasing importance in those application areas that require a high degree of automation and reliability of object recognition. For instance, typical applications include collision avoidance for vehicles/aircrafts or mobile robots, model-based detection and tracking of objects in close- and long-range environments, and the optimization and control of docking maneuvers.

1.3 Overview

MLS usually combines a LiDAR (light detection and ranging) device with highly accurate navigational sensors mounted on a mobile sensor platform (e.g., aircraft, vehicle). Typically, an IMU (inertial measurement unit) and GNSS receivers (global navigation satellite system, e.g., GPS, the Global Positioning System) are operated synchronously with a LiDAR scanning mechanism.

MLS is well suited to provide 3D measurements which allow direct comparison of geometric features, but additional requirements must be met by the data acquisition and data analysis if the laser scanner is used to support real-time operations, such as the surveillance of urban areas, terrain-referenced navigation, or detection of rapid changes. These applications require methods for immediate (on-the-fly) processing of range measurements instead of the classical offline treatment of recorded data. The intention to use such a sensor system for change detection implies that 3D reference data of the area in question have been acquired at an earlier date (t_1), so that currently (t_2) measured MLS data can be aligned and compared to these. In this paper, we address change detection in the case that both the reference data and the current data were/are acquired by an MLS system. In addition, we require this MLS system to allow access to the component's raw measurements, i.e., the range data, the scanning geometry, and the IMU/GNSS trajectory.

During the mission (t_2), all the new MLS measurements are to be (i) categorized, (ii) aligned and (iii) compared to the reference data. These three tasks are intended to be performed in line with the data acquisition, which means that the processing is done continuously on the acquired data stream instead of evaluating the complete point cloud. Regarding task (i), a fast segmentation method was described by Hebel and Stilla¹ that is based on scanline segmentation and grouping in consecutive scanlines. Matching objects, which are identified in both the current data and the reference data, can be used to correct absolute errors of the measured sensor position². Even if we have to deal with worse georeferencing accuracy and reliability due to uncorrected GNSS and/or IMU drift conditions, this terrain-referenced navigation ensures a permanent alignment of the data. In this paper, we focus on the comparison task (iii), and we start from the premise that the system calibration and data alignment issues are solved³.

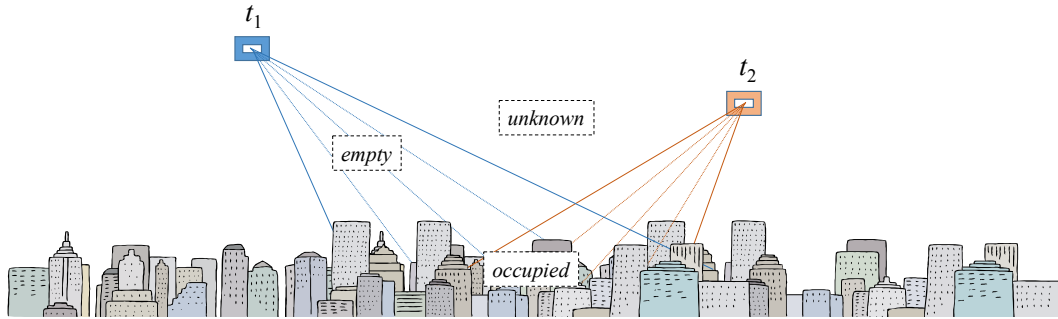


Figure 2. Illustration of multi-view and multi-temporal 3D data acquisition.

In our change detection approach, we include the sensor positions in the considerations. Thus, we retain the knowledge of *empty* space between the laser source and each reflecting 3D point (see Fig. 2). In robot mapping, such information is often managed in so-called occupancy grids⁴. We adapt some of these concepts for the use with MLS data. From a methodical point of view, the presented approach is designed for a future implementation for on-board processing, so MLS-system manufacturers are encouraged to utilize these concepts in their future development.

This paper is a summary of a more comprehensive journal paper⁵ and parts of a doctoral dissertation⁶. In addition, we present some recent activities and future plans of the working group⁷. In the next subsection, we give an overview of related work on change detection and occupancy grids. The methodology is explained in Section 2. A description of our different MLS setups (airborne, terrestrial) and experimental results can be found in Section 3. Finally, Section 4 presents our conclusions.

1.4 Related work

The use of laser scanning for change detection has been proposed, for instance, by Murakami et al.⁸ Typically, a digital surface model (DSM) is generated by interpolating the 3D points onto a 2D grid, and changes are detected by computing the difference of these DSM data. To increase the reliability of the change detection results, Vögtle and Steinle⁹ classify the laser points into the classes bare-earth, building, and vegetation. The analysis of multi-temporal MLS data is sometimes proposed to assess damage to buildings, e.g., after earthquakes. Hommel¹⁰ puts strong emphasis on the elimination of vegetation in the data, as this class of points could be misinterpreted, depending on the foliage state of the vegetation in the different data sets. A similar argumentation given by Rutzinger et al.¹¹ was also confirmed in our experiments. However, other applications are conceivable wherein the detection and analysis of urban vegetation are of prime importance¹². Recent studies on change detection methods and a detailed survey of related work are given by Matikainen et al.¹³ as well as Lindenbergh¹⁴.

Unlike the comparison of DSMs, the applications mentioned above require a different strategy for data processing. In robotics, similar boundary conditions occur in the simultaneous localization and mapping (SLAM) problem, if ranging sensors are used to generate global maps from local and uncertain sensor data (e.g., sonar, radar, or laser scanning). Most commonly, 2D maps that are horizontal projections of 3D space are taken as a basis. Moravec and Elfes⁴ were the first to represent these maps as 2D arrays of cells labeled *unknown*, *empty*, and *occupied*, with values ranging from 0 to 1 to define the “degree of certainty”. Puente et al.¹⁵ distinguish two different approaches to fuse information within such occupancy grids. These approaches are: (a) probabilistic estimation based on Bayes' theorem, and (b) the combination rule of the Dempster-Shafer theory of evidence^{16,17}. Detailed work on autonomous navigation of mobile robots by a combination of probabilistic occupancy grids with neural networks was done by Thrun¹⁸. Probabilistic occupancy grids have even been proposed for 3D object recognition¹⁹. Instead of a fixed-size 3D grid, Hornung et al.²⁰ use an adaptive octree representation together with a probabilistic occupancy estimation to generate volumetric 3D environment models.

The evidence theory of Dempster-Shafer^{16,17} is commonly used for data fusion. In the context of occupancy models, the Dempster-Shafer theory can substitute the probabilistic approach. There it has the advantage of evaluating conflicting information implicitly, which can be utilized to detect object movements in the scene²¹. In this paper, we evaluate such conflicts in multi-view and multi-temporal MLS data, which we organize in 3D grids. Instead of downsampling the data to the grid, it is possible to use the grid structure like a hash table, similar as it is described by Himmelsbach et al.²² for their 3D object perception system. A description of the strengths and weaknesses of a 3D-based approach is given in the next sections.

2. DATA ACQUISITION AND ANALYSIS

2.1 Direct georeferencing

Since an MLS system consists of several spatially separated parts, the mutual placement and alignment of these elements on the sensor platform are of great importance when combining the complementary information of all components. The lever arms of laser scanner, GNSS receiver and IMU are taken into account to transfer the positional coordinates to the laser scanner's center. The laser scanner itself is the core element of the MLS system. Typically, it makes use of the time-of-flight distance measurement principle, e.g. by estimating the range corresponding to the echo pulses as they can be found by constant fraction discrimination or full waveform analysis²³. Opto-mechanical scanning provides a specific scan pattern, in which a distance r_L measured at time t is georeferenced according to scanner geometry as well as position and orientation of the sensor. With the navigational information s (sensor position) and R_N (sensor orientation) relating to the laser scanner's center, r_L is directly georeferenced to a 3D point p in the following way:

$$p = s + R_N \circ R_S \circ r_L,$$

wherein s is the 3D position of the laser scanner at time t in a Cartesian geographic coordinate system (e.g., ECEF), r_L is the measured distance given as a Euclidean vector $(0, 0, r_L)^T$, R_S is a 3×3 rotation matrix that describes the scanning process, R_N is a 3×3 rotation matrix which describes the orientation of the laser scanner in 3D space, and p are the coordinates of the resulting "laser point". If r abbreviates the oriented distance vector $R_N \circ R_S \circ r_L$, this equation simplifies to

$$p = s + r.$$

The accuracy of the derived 3D point clouds is affected by several influencing factors, reflecting the complexity of an MLS system³. The overall point positioning accuracy is one of the crucial factors influencing the expectable exactness of the following change detection procedure.

2.2 Strategy for data processing

Two different stages are distinguished for MLS data acquisition and analysis. In stage I, a point database (reference) for time t_1 is built up and a 3D voxel grid that covers the complete area in question is filled with information. During stage II, it is decided whether current (t_2) MLS measurements confirm or contradict this information in the database. The voxel grid structure is used to store information on the proximity of laser "rays" (and points). Once established, this data structure enables to identify all candidates of old laser range measurements that may interfere with a new one. Furthermore, the cell size can be chosen comparatively wide (e.g., five times the average point-to-point distance), resulting in a moderate amount of data. Since the grid is only used as a search structure, the selection of the cell size has only minor impact on the results.

2.3 Generation of the database

Reference data captured at time t_1 contain the classified and co-registered laser measurements L of, for instance, multiple overlapping MLS scans. For each point p_i , the sensor position s_i and the range vector r_i are known. For storing the indices i in a spatial database, two voxel grids V_P and V_R with same size are defined. The cells of both grids are filled with indices from L (see Fig. 3). Each index i is included in a single cell of V_P according to the 3D position of the laser point p_i that corresponds to this index. Therefore, V_P simply represents a rasterization of the point cloud. Beyond that, V_R is used to store all indices of laser rays that traverse the voxels. Each cell in V_P or V_R can receive either none, one or multiple indices, depending on the number of laser points contained in this voxel, or depending on the number of laser rays that run through this voxel, respectively.

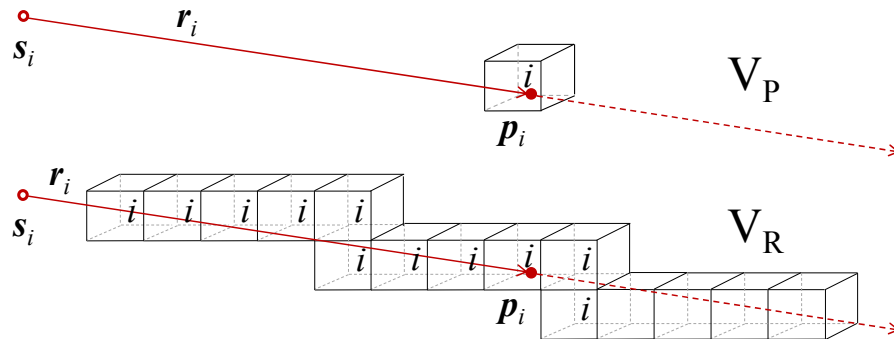


Figure 3. Filling the voxel grids V_P and V_R with the index of a laser measurement (i : index of the measurement).

2.4 Modeling the occupancy of space

For each single laser measurement, the occupancy of space can be assumed as *empty* between sensor and laser point, as *occupied* at the laser point itself, and as *unknown* everywhere else, especially behind the laser point in direction of the ray. In case multiple laser measurements affect the same area in space, the question comes up how the different and probably contradicting information can be fused. A possible strategy for fusion is based on the evidence theory by Dempster¹⁶ and Shafer¹⁷ which explicitly handles the state of uncertainty or vagueness. The application of this theory has some advantages in the context of the occupancy model: On one side, the uncertainty or vagueness allows to model occlusions and the resulting lack of information. On the other side, the combination rule of Dempster allows to assess conflicts of information which are of interest for automatic change detection. The occupancy of space can be described by functions assigning each position a so-called “belief mass” in the interval [0,1]. Fig. 4 shows the spatial modeling of positions q with transversal and longitudinal distance (d_x, d_y) related to a laser measurement p for the states *occupied*, *empty* and *unknown* by the mass functions $m_{q,p}(\{occ\})$, $m_{q,p}(\{emp\})$, and $m_{q,p}(U)$. In this model, the three parameters (λ, c, κ) determine the uncertainty of the laser rays and points and have to be chosen according to the physical properties and technical limitations of the MLS measurements (for details see Hebel et al.⁵). Especially $m_{q,p}(\{occ\})$ should be designed regarding the acquired point density and position accuracy which depend on the range resolution of the laser rangefinder, the precision of the scanner and the navigation system, and the size of the laser footprint.

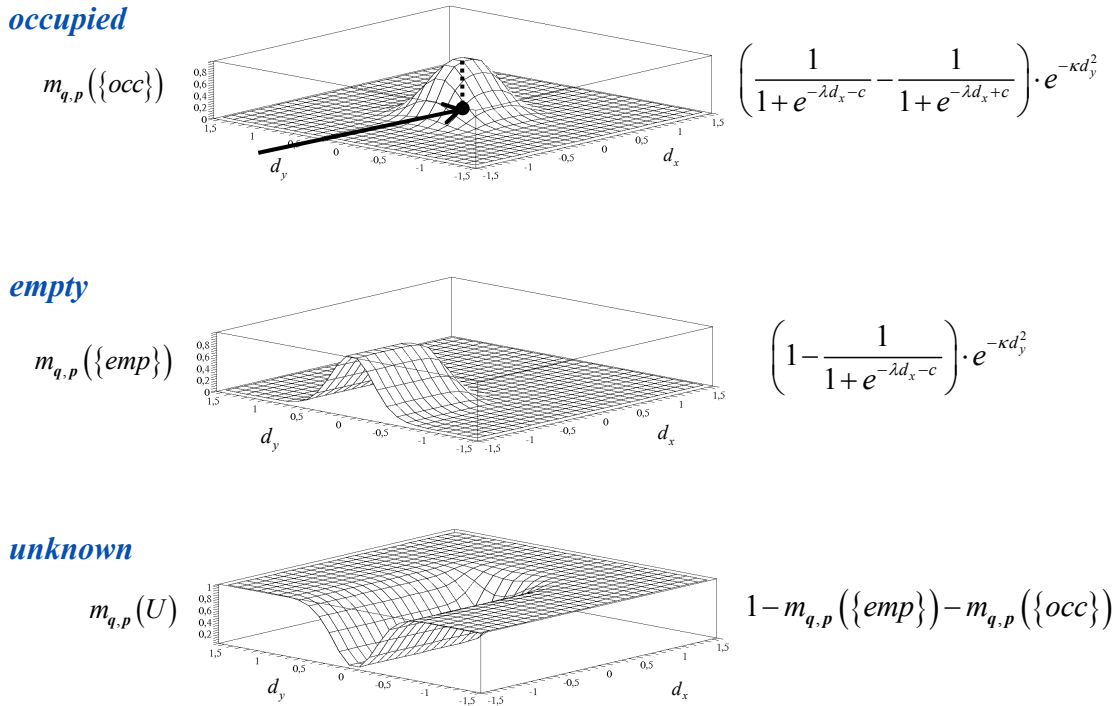


Figure 4. Belief masses *occupied*, *empty* and *unknown* in the vicinity of the laser point p .

2.5 Combination of evidences

In case of two or more laser rays and/or points which interfere, the corresponding mass assignments have to be combined. For calculation of a fused mass function, the combination rule of Dempster¹⁶ is used. In this process, a conflict C caused by two independent laser measurements p_1 and p_2 (*empty* in m_1 and *occupied* in m_2 , or *occupied* in m_1 and *empty* in m_2) is calculated by $C = m_{q,p1}(\{emp\}) \cdot m_{q,p2}(\{occ\}) + m_{q,p1}(\{occ\}) \cdot m_{q,p2}(\{emp\})$. Further details can be found in the paper of Hebel et al.⁵.

2.6 Detection of changes by space conflicts

During the phase of comparisons at time t_2 , the previous defined model of space occupancy is used to assess whether a new single MLS measurement $q = s_Q + r_Q$ confirms or contradicts the existing mass assignments in space. In this context, “existing assignment” means the local combination of mass functions (by Dempster’s rule of combination) which stem from MLS measurements of the reference data at time t_1 . Changes in the scene will be visible as contradictions or conflicts in space occupancy. Such conflicts occur in two cases, namely, if the laser ray (s_Q, r_Q) traverses a volume in space which is marked as *occupied* (Fig. 5b) or if the laser point q is measured in a volume in space which should be *empty* (Fig. 5a).

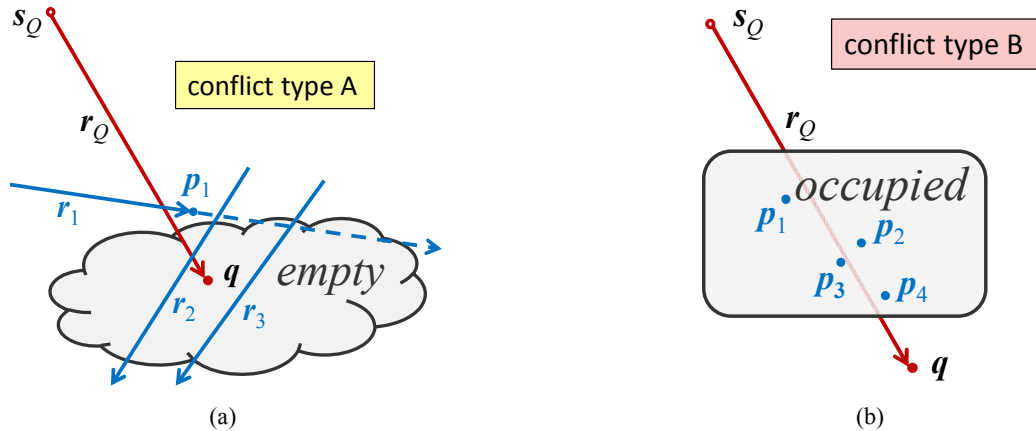


Figure 5. Conflicts between reference data (blue) and the current measurement (red). (a) Conflict type A: A new laser point q lies in a region that is labeled as *empty*, (b) conflict type B: A new laser “ray” (s_Q, r_Q) traverses an *occupied* space.

2.7 Considering additional attributes

The current model does not yet consider that some objects may lead to multiple reflections based on discontinuities of the surface or due to a small size. For instance, in case of a partial penetration of vegetation, a single pulse will label the same places along the measuring direction as *occupied* and *empty*. These self-induced conflicts will occur also for different laser measurements of the same unchanged space in case of vegetation. Furthermore, vegetation is subject to seasonal changes. If the detection of such changes is of minor importance, it is advisable to treat vegetation in a different way than ground level, buildings, or other man-made objects. Besides full waveform analysis²³, local principal component analysis (PCA) and region growing are common approaches to classify MLS points belonging to vegetation³. For these measurements an additional weighting factor is derived from local PCA that increases the amount of $m_{q,p}(U)$ and the dimensions of *occupied* space. Another obvious way to refine the model is to account for the orientation of continuous surfaces. If local PCA clearly reveals a local normal direction, $m_{q,p}(\{occ\})$ can be spread out along the detected surface. Again, the details can be found in the paper of Hebel et al.⁵.

3. EXAMPLES

3.1 Airborne laser scanning of urban areas (helicopter)

Airborne laser scanning (ALS) is a variant of mobile laser scanning that uses a flying sensor platform (e.g., a helicopter). ALS data that were analyzed for this study were acquired during field campaigns in 2008 and 2009, using a RIEGL LMS-Q560 laser scanner (version 2006) in combination with an Applanix POS AV 410 inertial navigation system. All sensors were attached to a helicopter of type Bell UH-1D (cf. Fig. 6). This experimental setup²⁴ lacks online data access, so we had to simulate the on-the-fly data analysis: All experiments described in this section were conducted in a post-processing mode based on the stream of recorded raw data. With our configuration and settings, each scan line of the laser scanner covered a field of view of 60° subdivided into 1000 angular steps. The inclination angle of the laser scanner was set to 45° while flying with the helicopter's nose pitched down. Due to aviation security reasons, the minimum flight level had to be restricted to 1000 ft. These boundary conditions led to laser strips with a width of 500 m and an average point-to-point distance of 0.5 m. The cell size of V_R and V_P was chosen to be $2 \times 2 \times 2 \text{ m}^3$, resulting in two cell arrays of the dimensions $300 \times 300 \times 50$ (which corresponds to $600 \times 600 \times 100 \text{ m}^3$) to cover the area in question.

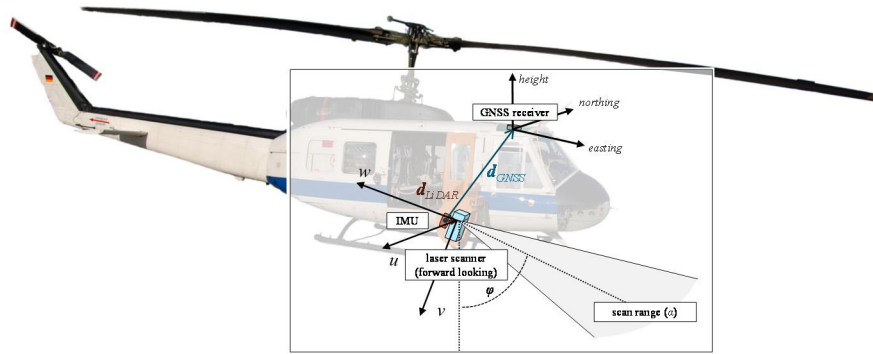


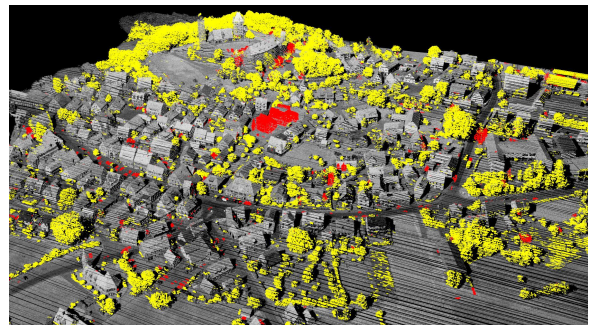
Figure 6. Experimental setup used for airborne laser scanning (ALS).

In April 2008, the test site Abenberg (Bavaria, Germany) was covered by four strips in a cross pattern, resulting in an accumulated point cloud which includes 5,400,000 points with an average point density of 16 pts/m². Fig. 7a shows a rendered visualization of these reference data, where each point is gray-value coded according to the echo amplitude, which is derived from full waveform analysis of the backscattered pulse²³.

The test site was scanned again in August 2009, using the same sensors and a similar setting. Based on the recorded data stream of a single strip from south to north (1,500,000 points), the methods described in the previous sections were successfully applied. The parameters of the functions shown in Fig. 4 were set to $\lambda=12$, $c=5$ and $\kappa=8$. Fig. 7b shows conflicts of type B (objects that have disappeared) in red and the conflicts of type A (objects that have appeared) in yellow. In this example, vegetation obviously causes a lot of type A conflicts, which can be ascribed to seasonal influences (April vs. August). In case we want to focus on man-made changes, according to section 2.7 additional attributes and a classification of reference data into *ground*, *vegetation*, and *building* can be used to reduce changes induced by vegetation. Details of such a result are shown in Fig. 7e. In addition to the previous color-coding, green points now indicate that these are (most likely) part of an unchanged building. The remaining conflicts are mainly caused by moved cars, newly constructed and demolished buildings.



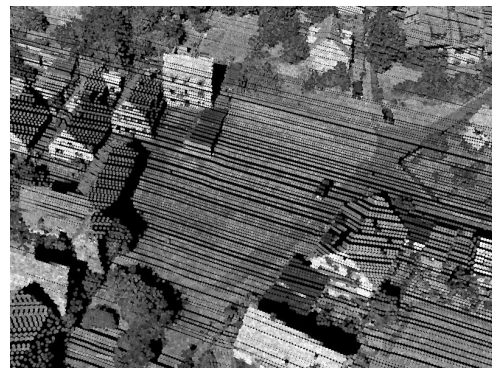
(a) Reference data: Abenberg, 18.04.2008



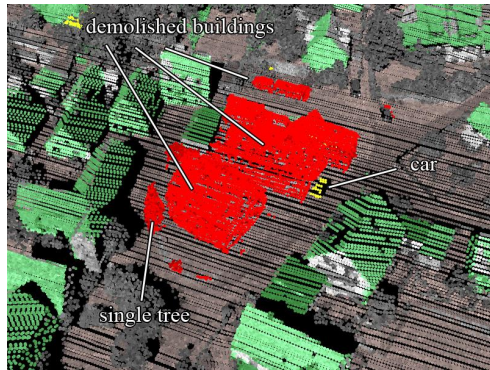
(b) Comparison: Abenberg, 31.08.2009



(c) Details Abenberg 2008



(d) Details Abenberg 2009



(e) Considering additional attributes

Details of the change detection results:

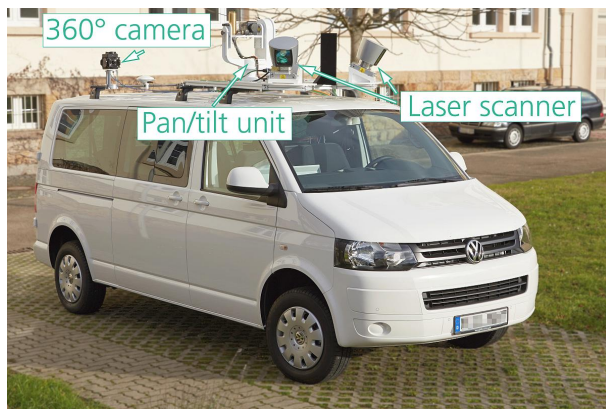
- Conflict type A (appeared)
- Conflict type B (disappeared)
- Confirmed planar areas, parts of buildings
- Unchanged

Figure 7. Results and different types of detected changes, e.g., demolition of buildings, moved cars.

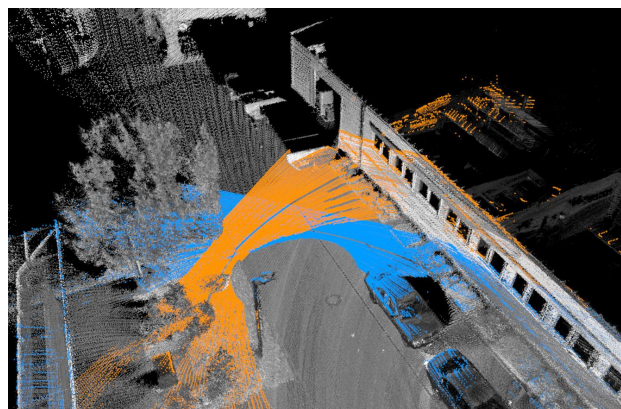
3.2 Mobile terrestrial laser scanning (vehicle)

In the near future, modern vehicles will be equipped with a variety of sensors, computers, and communication systems, for example to implement driver assistance functions. On the civilian market, this development is largely driven by a growing interest in safety and comfort. Additionally, the military has an increasing demand for situation-awareness capabilities in their vehicles. These trends have become well established in the scientific community, and the current work of the group is focused on vehicle-based data acquisition and processing.

“MODISSA” (Mobile Distributed Situation Awareness) is the IOSB’s realization of an experimental platform for hardware evaluation and software development in the contexts of automotive safety, security, and military applications. Example applications for its sensors are obstacle detection and avoidance, traffic monitoring, acquisition of 3D models, change detection, as well as target location, target tracking, target designation and target handoff between vehicles. MODISSA is based on a Volkswagen van T5 that has been equipped with a broad range of sensors and contains hardware for complete raw data capture, real-time data analysis, and immediate data visualization on in-car displays (cf. Fig. 8a). The VW van carries several sensors on a roof rack, and a power supply as well as operational electronics inside. The current sensor configuration includes two rotating Velodyne HDL-64E laser scanners, an omnidirectional camera, and two cameras on a pan-tilt unit (one visual-range camera and one microbolometer infrared camera). The laser scanners are located ahead of both roof rack bars over the front corners of the vehicle roof, and are positioned on a wedge with a 25 degree angle to the horizontal, sloping to the front outside at a 45 degree angle. This configuration guarantees a good coverage of the roadway in front of the car and allows scanning of building facades alongside and behind it (see Fig. 8b). A vertical plate between the laser scanners serves to shield these from mutual direct laser radiation.



(a)



(b)

Figure 8. (a) The MODISSA platform enables mobile sensor data acquisition, sensor data analysis and mobile demonstrations. (b) Accumulated 3D data acquired with the two Velodyne laser scanners (blue and orange for visualization of currently added point clouds).

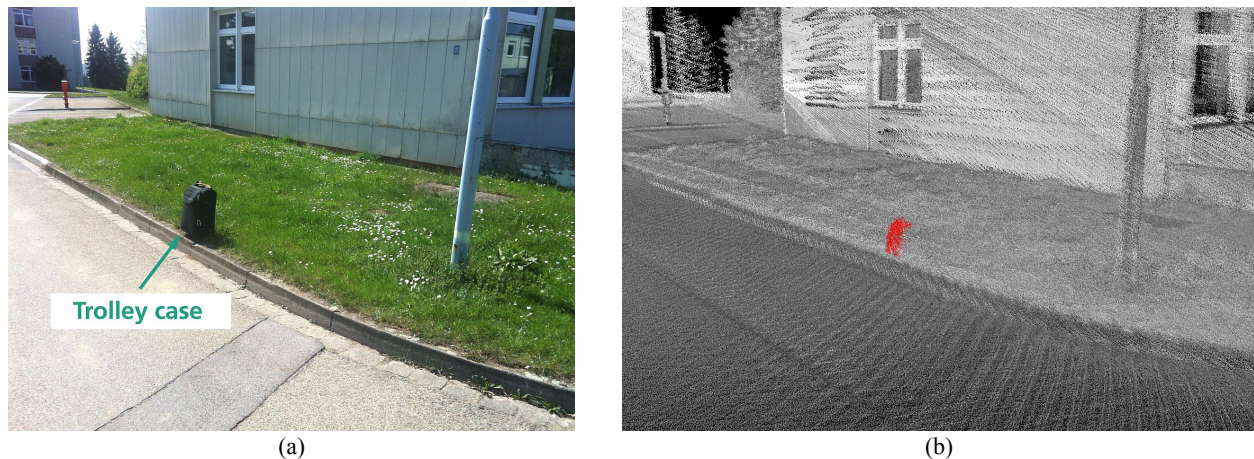


Figure 9. (a) Test scenario for change detection with MLS data: a trolley case at the roadside. (b) Result of automatic change detection: space conflicts shown in red.

Methods like those described in Section 2 can be applied to MLS data acquired by the two Velodyne laser scanners of MODISSA. Fig. 9 shows results for a test scenario with intentionally prepared changes: First, reference data were acquired of the roadway, its surroundings and building facades along a road. Second, a trolley case was placed on the roadside to simulate an IED-like object (Fig. 9a). Third, new MLS data were acquired during the next passage on that road and changes were detected automatically (Fig. 9b). To achieve this result, the current implementation of the change detection method is based on a 3D occupancy grid with a $10 \times 10 \times 10 \text{ cm}^3$ cell size. Future work will concentrate on the full implementation of the methods from Section 2 and the optimization of the parameters in this approach to achieve an even lower false alarm rate.

4. CONCLUSION

The experiments described in Section 3 demonstrate that spatial changes can be reliably detected with multitemporal MLS data, provided that the data are properly aligned. The minimum size of detectable changes is limited by the point density and the respective point positioning accuracy, which need to be modeled correctly by means of the parameters λ, c, κ (in Section 3.1) or the voxel size (in case of a standard 3D occupancy grid, Section 3.2). A reasonable setting represents a compromise between the achievable level of detail and the tolerance against data misalignment. As to be expected, a small point density and/or discrepancies between the different data sets result in a low level of detail. If the discrepancies are small, we recommend to set the parameters (λ, c, κ) such that the FWHM of $m_{q,p}(\{occ\})$ amounts to approximately twice the average point-to-point distance, so that the measurements will have a significant overlap. In case of large discrepancies, the occupancy of space at the position of p needs to be modeled even broader in order to smooth the registration errors.

Overall, we were able to detect changes of approximately $1 \times 1 \times 1 \text{ m}^3$ with the ALS system and expect to detect changes of $20 \times 20 \times 20 \text{ cm}^3$ with the vehicle-based MLS system. However, these statements are specific to our experimental setup and specific to the underlying circumstances during our field campaigns (e.g., local point density etc.). The presented methodology is independent of hardware and survey characteristics, and it can easily be adapted to any airborne or terrestrial laser scanning system. The change detection example in Section 3.2 represents a first and preliminary test of the MODISSA platform. In future work, we will implement the described methods on its on-board hardware. In addition, we will realize other extensive applications on the MODISSA platform, such as pedestrian detection, target detection and target handoff applications, as well as wide-area 3D model acquisition.

REFERENCES

- [1] Hebel, M. and Stilla, U., "Pre-classification of points and segmentation of urban objects by scan line analysis of airborne LiDAR data," International Archives of the Photogrammetry, Remote Sensing and Spatial Information Sciences 37 (B3a), 105-110 (2008).

- [2] Hebel, M. and Stilla, U., "LiDAR-supported navigation of UAVs over urban areas," *Surveying and Land Information Science, Journal of the American Congress on Surveying and Mapping* 70, 139-149 (2010).
- [3] Hebel, M. and Stilla, U., "Simultaneous calibration of ALS systems and alignment of multiview LiDAR scans of urban areas," *IEEE Transactions on Geoscience and Remote Sensing* 50 (6), 2364-2379 (2012).
- [4] Moravec, H. P. and Elfes, A., "High Resolution Maps from Wide Angle Sonar," *Proceedings of the IEEE International Conference on Robotics and Automation*, 116-121 (1985).
- [5] Hebel, M., Arens, M. and Stilla, U., "Change detection in urban areas by object-based analysis and on-the-fly comparison of multi-view ALS data," *ISPRS Journal of Photogrammetry and Remote Sensing* 86, 52-64 (2013).
- [6] Hebel, M., "Change detection in urban areas by object-based analysis and on-the-fly comparison of multi-view ALS data," *Doctoral Thesis (in German), TUM*, <<http://d-nb.info/1031513159/34>>, 156 p. (2012).
- [7] Hebel, M., "Object recognition in 3D data," *Group Description, Department Object Recognition (OBJ), Fraunhofer IOSB*, <<http://www.iosb.fraunhofer.de/servlet/is/20835/>>, (2014).
- [8] Murakami, H., Nakagawa, K., Hasegawa, H., Shibata, T. and Iwanami, E., "Change detection of buildings using an airborne laser scanner," *ISPRS Journal of Photogrammetry and Remote Sensing* 54 (2-3), 148-152 (1999).
- [9] Vögtle, T. and Steinle, E., "Detection and recognition of changes in building geometry derived from multitemporal laserscanning data," *International Archives of the Photogrammetry, Remote Sensing and Spatial Information Sciences* 35 (B2), 428-433 (2004).
- [10] Hommel, M., "Verification of a building damage analysis and extension to surroundings of reference buildings," *International Archives of the Photogrammetry, Remote Sensing and Spatial Information Sciences* 38 (3/W8), 18-23 (2009).
- [11] Rutzinger, M., Rüb, B., Höfle, B. and Vetter, M., "Change detection of building footprints from airborne laser scanning acquired in short time intervals," *International Archives of Photogrammetry, Remote Sensing and Spatial Information Sciences* 38 (7b), 475-480 (2010).
- [12] Rutzinger, M., Höfle, B., Hollaus, M. and Pfeiffer, "Object-based point cloud analysis of full-waveform airborne laser scanning data for urban vegetation classification," *Sensors* 8 (8), 4505-4528 (2008).
- [13] Matikainen, L., Hyyppä, J., Ahokas, E., Markelin L. and Kaartinen H., "Automatic detection of buildings and changes in buildings for updating of maps," *Remote Sensing* 2 (5), 1217-1248 (2010).
- [14] Lindenbergh, R., "Engineering Applications: structural monitoring and change detection," in Vosselman, G. and Maas, H.-G. (eds.), "Airborne and terrestrial laser scanning," *CRC Press LLC*, 243-261 (2010).
- [15] Puente, E.A., Moreno, L., Salichs, M.A. and Gachet, D., "Analysis of data fusion methods in certainty grids - application to collision danger monitoring," *Proceedings of the IEEE International Conference on Industrial Electronics, Control and Instrumentation*, 1133-1137 (1991).
- [16] Dempster, A.P., "Upper and lower probabilities induced by a multivalued mapping," *Annals of Mathematical Statistics* 38 (2), 325-339 (1967).
- [17] Shafer, G., "A mathematical theory of evidence," *Princeton University Press* (1976).
- [18] Thrun, S., "Learning metric-topological maps for indoor mobile robot navigation," *Artificial Intelligence* 99 (1), 21-71 (1998).
- [19] Yapo, T.C., Stewart, C.V. and Radke, R.J., "A probabilistic representation of LiDAR range data for efficient 3D object detection," *IEEE Conference on Computer Vision and Pattern Recognition, Workshop CVPRW'08* (2008).
- [20] Hornung, A., Wurm, K.M., Bennewitz, M., Stachniss, C. and Burgard, W., "OctoMap: An efficient probabilistic 3D mapping framework based on octrees," *Autonomous Robots* 34, 189-206 (2013).
- [21] Moras, J., Cherfaoui, V. and Bonnifait, P., "A LiDAR perception scheme for intelligent vehicle navigation," *Proceedings of the IEEE 11th International Conference on Control, Automation, Robotics and Vision ICARCV* (2010).
- [22] Himmelsbach, M., Müller, A., Lüttel, T. and Wünsche, H.-J., "LiDAR based 3D object perception," *Proceedings of the 1st International Workshop on Cognition for Technical Systems*, 1-7 (2008).
- [23] Stilla, U. and Jutzi, B., "Waveform Analysis for Small-Footprint Pulsed Laser Systems," in Shan J. and Toth C. (eds.), "Topographic Laser Ranging and Scanning: Principles and Processing," *Chapter 7, CRC Press* (2009).
- [24] Schatz, V., "Synchronised data acquisition for sensor data fusion in aerial surveying," *Proceedings of the 11th International Conference on Information Fusion*, 1125-1130 (2008).